Performance Analysis of Ultra-Wideband Rake Receivers with Channel Delay Estimation Errors

Hongsan Sheng, Roy You, Alexander M. Haimovich
Center for Communications and Signal Processing Research
New Jersey Institute of Technology
Newark, NJ 07102
Email: {hs23, you, haimovic}@njit.edu

***Abstract*— The performance of an ultra-wideband (UWB) Rake receiver over a sparse multipath channel with an exponential power delay profile is investigated in the presence of path delay estimation errors. An exact expression of the bit error probability accounting for both tap misalignement and missing-path errors is obtained. Also obtained are an approximate simpler expression and upper/lower bounds. The exact expression is compared with simulations and is shown to be in good agreement.**

***Index Terms*— UWB, imperfect channel estimate, path delay estimation, Rake receiver design**

I. Introduction

In this paper, we investigate the effect of channel estimation errors for impulse radio (IR) ultra-wideband (UWB) receivers. One attractive feature of IR-UWB is the ability to resolve multipath and use the path information for channel diversity gains [1]. A Rake receiver can be employed to exploit the diversity by capturing the energy spread by the multipath channel. With perfect knowledge of channel state information and in the presence of additive white Gaussian noise, the Rake receiver with maximum ratio combining (MRC) maximizes the output signal-to-noise ratio (SNR). However, in practice, the paths of the multipath channel must be estimated and the estimation error, especially the path delay error, will lead to performance loss. For IR-UWB, the problem is further exacerbated because of the extremely short duration pulses.

For the UWB multipath channel with sparse paths, the analysis of the effect from the path delay estimate is different from that of symbol timing jitter in narrowband systems. Because the pulse duration is short, the path delay error can either lead to a small offset producing a misalignment error (similar to timing jitter), or make the receiver miss the path completely if the offset is greater than the pulse width [2]. In previous studies ([3] and [4]), only the misalignment error due to timing jitter was considered. In this paper, we analyze the impact of path delay errors on the system performance considering both the misalignment error and the missing-path error over a dispersive multipath channel with an exponential power delay profile (PDP).

It has been shown that the variance of the path delay estimate error is a function of the path SNR, bandwidth of the signal, and observation time [5]. In previous papers ([3] and [4]), same variances of the estimate error were assumed for all paths and all SNR. We take into account the effect from the path SNR and the number of pilot symbols used to improve the path SNR in estimation. An exact expression of the bit error probability (BEP) is developed accounting for the path delay estimation error. The expression is shown to be in good agreement with Monte Carlo simulations. For small path delay estimation errors, a simpler approximation is also derived and shown to be close to the exact BEP. By an alternative method using the SNR at the output of the combiner, an upper bound and a lower bound of the BEP are also obtained.

The rest of this paper is organized as follows. In Section II, the signal model is introduced and the channel estimation method is described. Section III presents the detailed derivation of BEP considering the path delay estimation error for Rake receivers using MRC. An approximation is obtained when the path delay estimation error is small. Furthermore, an upper and a lower bound are given for comparison by an alternative method. In Section IV, results of Monte Carlo simulations are shown to be in close match with the analytical results. Section V provides the conclusions.

II. System Model

A. Signal Model

The impulse radio UWB system transmission model is shown in Fig. 1. A binary bit stream is transmitted over a multipath channel and each data bit is modulated by a very short duration pulse. Although other pulses can be used, to facilitate exact-form analytical results, we use a rectangular pulse $q(t)$ with a pulse width T_p and energy E_b,

$$q(t) = \begin{cases} \sqrt{\frac{E_b}{T_p}}, & 0 \le t \le T_p \\ 0, & \text{else.} \end{cases} \tag{1}$$

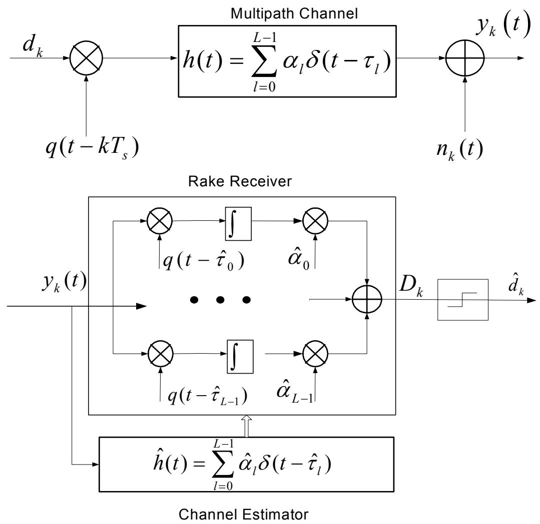

Fig. 1. A complete impulse radio transmission model over a multipath channel.

The multipath channel is given by

$$h\left(t\right)=\sum_{l=0}^{L-1}\alpha_l\delta\left(t-\tau_l\right), \tag{2}$$

where L is the number of multipath, α_l and τ_l are the path gain and delay for the l-th path, respectively. We assume the channel is quasi-static (fixed over the duration of a packet), hence the channel parameters are modeled as deterministic, but unknown. As shown in Fig. 2, the channel model is an FIR filter with an exponential PDP, $\alpha_l^2=\Omega_l=\Omega_0\exp\left(-\tau_l/\tau_{\max}\right)$. Ω_0 is chosen in such a way as to ensure that average received power is unity [6]. The sign of α_l is equiprobable ± 1. The negative sign accounts for signal inversion due to reflections. The path distribution is deterministic and sparse. By sparse we mean that there is no inter-pulse interference at the channel output.

Consider biphase modulation, and the received signal is given by

$$\begin{aligned} y\left(t\right) &= dq(t)\otimes h(t)+n(t) \\ &= d\sum_{l=0}^{L-1}\alpha_l q(t-\tau_l)+n(t), \end{aligned} \tag{3}$$

where $d\in\{\pm 1\}$ with equal probability denotes the binary bit, $\otimes$ represents the convolution operation, and the noise $n(t)$ is white, Gaussian with zero-mean and two-sided power spectral density of $N_0/2$. We assume the symbol duration is larger than the maximum delay spread such that the inter-symbol interference can be neglected. L branch correlators are used for the Rake receiver, where the received signal is correlated with suitable delayed reference pulses using the estimated path delays. The path amplitude estimates are used as the weights of the linear combiner for MRC. In the next subsection, the channel estimation method is described and the estimation error model is discussed.

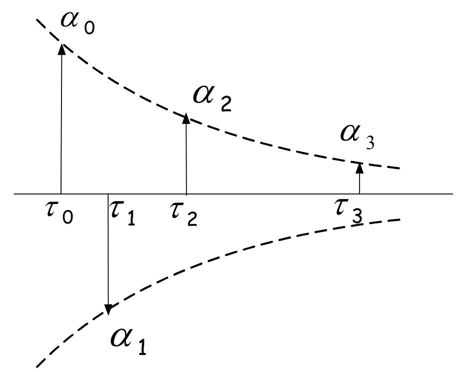

Fig. 2. A UWB multipath channel impulse response with an exponential power delay profile and sparse tap delays.

B. Channel Estimation

A pilot-aided channel estimation is used, whereas each packet in the observation consists of a preamble of M pilot symbols followed by the information data. Channel paths are estimated using multiple pilot symbols and maximum likelihood estimation [7]. The outputs of the correlator are over-sampled to improve the resolution of the path delay estimation. The estimate of the path delay can be expressed as $\widehat{\tau}_l=\tau_l+\epsilon_l T_p$, where ϵ_l is the estimation error normalized to the pulse width. Estimation errors of the paths are assumed mutually independent. The error is modeled with a Gaussian pdf [8]

$$p\left(\epsilon_l\right)=\frac{1}{\sqrt{2\pi}\sigma_{\epsilon_l}}\exp\left(-\frac{\epsilon_l^2}{2\sigma_{\epsilon_l}^2}\right). \tag{4}$$

where $\sigma_{\epsilon_l}^2$ is the variance of the error for the l-th path and defined in the sequel. Using this model, we take into account not only the misalignment error ($|\epsilon_l|\leq 1$), but also the missing-path error ($|\epsilon_l|>1$).

We are using the Cramér-Rao bound as the variance of the delay estimate. It can be expressed [9]

$$\mathrm{Var}\left(\widehat{\tau}_l\right)=\frac{1}{\frac{2E_b}{N_0}\alpha_l^2 M\rho^2}, \tag{5}$$

where $\rho^2\approx 1/T_p^2$ is the mean square bandwidth of the pulse. Then the variance of the normalized delay error is given by

$$\sigma_{\epsilon_l}^2=\frac{1}{\frac{2E_b}{N_0}\alpha_l^2}\frac{1}{M}. \tag{6}$$

Errors will occur in the path gain as well. However, in this paper, we assume that path gain errors are negligible. Thus, the estimated channel impulse response is given by

$$\widehat{h}(t) = \sum_{l=0}^{L-1} \widehat{\alpha}_l \delta(t - \widehat{\tau}_l), \quad (7)$$

where $\widehat{\alpha}_l \approx \alpha_l$. In the next section, we develop the BEP analysis taking into account path delay errors.

III. BEP Analysis

At the receiver, the time dispersed signal at the channel output is processed by MRC. From (3), the decision variable at the output of the linear combiner is given by

$$\begin{aligned} D &= \frac{1}{E_b} \int_{-\infty}^{+\infty} y(t) \sum_{l=0}^{L-1} \alpha_l q(t - \widehat{\tau}_l)\, dt \\ &= d \sum_{l=0}^{L-1} \alpha_l^2 \mu_q(\epsilon_l T_p) + \sum_{l=0}^{L-1} n_l, \end{aligned} \quad (8)$$

where the term $1/E_b$ is used to simplify the expression without affecting the decision, $\mu_q(\tau)$ is the autocorrelation function of the UWB pulse normalized to its energy

$$\mu_q(\tau) = \frac{\int_{-\infty}^{\infty} q(t) q(t-\tau) dt}{\int_{-\infty}^{\infty} q^2(t) dt} = \begin{cases} 1 - \frac{|\tau|}{T_p}, & |\tau| \le T_p \\ 0, & \text{else.} \end{cases} \quad (9)$$

Conditioned on the path gain, the noise

$$n_l = \frac{\alpha_l}{E_b} \int_{-\infty}^{\infty} n(t) q(t - \widehat{\tau}_l)\, dt \quad (10)$$

is a Gaussian random variable with zero mean and variance of $\frac{N_0}{2E_b}\alpha_l^2$. The decision rule is $D \underset{-1}{\overset{1}{\gtrless}} 0$. We derive the exact BEP and its upper and lower bounds next.

A. Exact BEP Analysis

The BEP is obtained by using the relation between cumulative distribution function (CDF) and the characteristic function (CF) of the decision variable. The Gil-Pelaez lemma in [10] indicates that a one dimensional CDF $F(x)$ is a function of its corresponding CF $\Psi(\omega)$ as expressed in

$$F(x) = \frac{1}{2} - \frac{1}{\pi} \int_0^{\infty} \frac{\mathrm{Im}\left[\Psi(\omega) \exp(-j\omega x)\right]}{\omega} d\omega. \quad (11)$$

Assume that $d = 1$ is transmitted, the BEP is

$$P_e = \Pr(D < 0) = \frac{1}{2} - \frac{1}{\pi} \int_0^{\infty} \frac{\mathrm{Im}\left[\Psi_D(\omega)\right]}{\omega} d\omega. \quad (12)$$

Conditioned on each channel realization, the CF of the decision variable is given by

$$\begin{aligned} \Psi_D(\omega) &= E\left[e^{j\omega D}\right] \\ &= \prod_{l=0}^{L-1} E\left[e^{j\omega \alpha_l^2 \mu_q(\epsilon_l T_p)}\right] \prod_{l=0}^{L-1} E\left[e^{j\omega n_l}\right] \\ &= \prod_{l=0}^{L-1} \Psi_{s_l}(\omega) \prod_{l=0}^{L-1} \Psi_{n_l}(\omega) \end{aligned} \quad (13)$$

with the assumption of mutually independent ϵ_l and n_l. The CF of the noise is

$$\prod_{l=0}^{L-1} \Psi_{n_l}(\omega) = \exp\left[-\frac{\omega^2 \sum_{l=0}^{L-1} \alpha_l^2}{4E_b/N_0}\right]. \quad (14)$$

Let

$$\Phi(x) = \frac{2}{\sqrt{\pi}} \int_x^{\infty} e^{-t^2} dt \quad (15)$$

be the complementary error function [11, Ch. 2]. From (4) and (6), we obtain

$$\begin{aligned} \Psi_{s_l}(\omega) &= 2\int_0^1 e^{j\omega\alpha_l^2(1-\epsilon_l)} p(\epsilon_l) d\epsilon_l + \Phi\left(\frac{1}{\sqrt{2}\sigma_{\epsilon_l}}\right) \\ &= \exp\left(-\frac{\omega^2\alpha_l^2}{M \cdot 4E_b/N_0}\right) \exp\left(j\omega\alpha_l^2\right) \\ &\quad \cdot \left[\Phi\left(\frac{j\omega\sigma_{\epsilon_l}^2\alpha_l^2}{\sqrt{2}\sigma_{\epsilon_l}}\right) - \Phi\left(\frac{1 + j\omega\sigma_{\epsilon_l}^2\alpha_l^2}{\sqrt{2}\sigma_{\epsilon_l}}\right)\right] \\ &\quad + \Phi\left(\frac{1}{\sqrt{2}\sigma_{\epsilon_l}}\right), \end{aligned} \quad (16)$$

where the last equality is obtained by [12, p. 354, 3.322]. By expressing

$$\Phi\left(\frac{j\omega\sigma_{\epsilon_l}^2\alpha_l^2}{\sqrt{2}\sigma_{\epsilon_l}}\right) - \Phi\left(\frac{1 + j\omega\sigma_{\epsilon_l}^2\alpha_l^2}{\sqrt{2}\sigma_{\epsilon_l}}\right) = C_I(\omega) + jC_Q(\omega), \quad (17)$$

where $C_I(\omega)$ and $C_Q(\omega)$ respectively denote the real and imaginary parts, (16) becomes

$$\Psi_{s_l}(\omega) = e^{-\frac{\omega^2\alpha_l^2}{M \cdot 4E_b/N_0}} \left[U_l(\omega) + W_l(\omega) + jV_l(\omega)\right], \quad (18)$$

where

$$\begin{aligned} U_l(\omega) &= C_I(\omega)\cos\left(\omega\alpha_l^2\right) - C_Q(\omega)\sin\left(\omega\alpha_l^2\right) \\ V_l(\omega) &= C_I(\omega)\sin\left(\omega\alpha_l^2\right) + C_Q(\omega)\cos\left(\omega\alpha_l^2\right) \\ W_l(\omega) &= \Phi\left(\frac{1}{\sqrt{2}\sigma_{\epsilon_l}}\right)\exp\left(\frac{\omega^2\alpha_l^2}{M \cdot 4E_b/N_0}\right). \end{aligned}$$

Thus, we have

$$\begin{aligned} \frac{\mathrm{Im}\,\Psi_{D_k}(\omega)}{\omega} &= \exp\left(-\frac{\omega^2\left(1 + \frac{1}{M}\right)\sum_{l=0}^{L-1}\alpha_l^2}{4E_b/N_0}\right) \\ &\quad \cdot \frac{R(\omega)\sin\left[\Theta(\omega)\right]}{\omega}, \end{aligned} \quad (19)$$

with

$$R(\omega) = \prod_{l=0}^{L-1} \sqrt{[U_l(\omega) + W_l(\omega)]^2 + V_l^2(\omega)}, \quad (20)$$

$$\Theta(\omega) = \sum_{l=0}^{L-1} \tan^{-1}\left(\frac{V_l(\omega)}{U_l(\omega) + W_l(\omega)}\right). \quad (21)$$

If we define

$$A = \frac{\left(1 + \frac{1}{M}\right)\sum_{l=0}^{L-1} \alpha_l^2}{4E_b/N_0}, \quad (22)$$

$$f(\omega) = \frac{R(\omega)\sin[\Theta(\omega)]}{\omega}, \quad (23)$$

from (12), the BEP is given by

$$P_e = \frac{1}{2} - \frac{1}{\pi}\int_0^\infty \exp\left(-A\omega^2\right) \cdot f(\omega)\, d\omega. \quad (24)$$

Since $\exp\left(-A\omega^2\right)$ can be considered as a weight function to $f(\omega)$, the integral in (24) is interpreted as a weighted average of $f(\omega)$ over its range [13, p. 22]. This Gauss type integral can be calculated using the Hermite formula [13, p. 224]. Thus the BEP can be expressed in closed-form

$$P_e = \frac{1}{2} - \frac{1}{\pi\sqrt{A}}\sum_{i=1}^{N} H_{x_i} f\left(\frac{x_i}{\sqrt{A}}\right), \quad (25)$$

where N is the order of the Hermite polynomial, x_i and H_{x_i} are respectively the zeros and weight factors of the i-th order Hermite polynomial which are tabulated in [14, p. 924, Table 25.10]. Typically, $N = 20$ is sufficient for good accuracy.

Note that P_e in (25) is conditioned on each channel realization. For a fading channel with random $\{\alpha_l\}$, the BEP can be obtained by averaging P_e in (25) over the available channel realizations.

A somewhat simpler expression for the BEP can be obtained by neglecting $W_l(\omega)$ in (18). Indeed, for small σ_{ϵ_l}, $\Phi\left(\frac{1}{\sqrt{2}\sigma_{\epsilon_l}}\right) \approx 0$. So $R(\omega)$ in (20) and $\Theta(\omega)$ in (21) can be simplified as

$$\overline{R}(\omega) = \prod_{l=0}^{L-1} \sqrt{C_I^2(\omega) + C_Q^2(\omega)}$$

$$\overline{\Theta}(\omega) = \sum_{l=0}^{L-1} \tan^{-1}\frac{C_I(\omega)\sin\omega\alpha_l^2 + C_Q(\omega)\cos\omega\alpha_l^2}{C_I(\omega)\cos\omega\alpha_l^2 - C_Q(\omega)\sin\omega\alpha_l^2}.$$

Substituting these in (23), we have

$$\overline{f}(\omega) = \frac{\overline{R}(\omega)\sin\left[\overline{\Theta}(\omega)\right]}{\omega}. \quad (26)$$

An approximate expression of the BEP is obtained from (24)

$$P_e \approx \frac{1}{2} - \frac{1}{\pi}\int_0^\infty \exp\left(-A\omega^2\right) \cdot \overline{f}(\omega)\, d\omega. \quad (27)$$

The integral is also a Gauss type and can be calculated by the Hermite formula as in (25).

If we consider only the misalignment error, the probability density function of the delay error is a truncated Gaussian with

$$p(\epsilon_l) = \begin{cases} \frac{\exp\left[-\epsilon_l^2/\left(2\sigma_{\epsilon_l}^2\right)\right]}{\left[1-\Phi\left(1/\sqrt{2}/\sigma_{\epsilon_l}\right)\right]\sqrt{2\pi}\sigma_{\epsilon_l}}, & |\epsilon_l| \leq 1 \\ 0, & \text{else.} \end{cases} \quad (28)$$

Then (19) becomes

$$\frac{\operatorname{Im}\Psi_{D_k}(\omega)}{\omega} = \frac{\exp\left(-A\omega^2\right) \cdot \overline{f}(\omega)}{1 - \Phi\left(1/\sqrt{2}/\sigma_{\epsilon_l}\right)}, \quad (29)$$

where A and $\overline{f}(\omega)$ are defined in (22) and (26) respectively. Substituting (29) in (12), the BEP for this case can be calculated.

B. BEP Bounds

Lower and upper bounds to the BEP can be derived by starting with the SNR at the output of the Rake combiner [15]. From (8), conditioned on the estimate of delay $\widehat{\tau}_l$, the SNR at the combiner output is given by

$$\gamma_t = \frac{2E_b}{N_0}\frac{\left[\sum_{l=0}^{L-1} \alpha_l^2 \mu_q(\epsilon_l T_p)\right]^2}{\sum_{l=0}^{L-1} \alpha_l^2}. \quad (30)$$

Next, we derive lower and upper bounds.

1) Lower Bound: By the Cauchy-Schwartz inequality,

$$\left[\sum_{l=0}^{L-1} \alpha_l^2 \mu_q(\epsilon_l T_p)\right]^2 \leq \left[\sum_{l=0}^{L-1} \alpha_l^2\right]\left[\sum_{l=0}^{L-1} \alpha_l^2 \mu_q^2(\epsilon_l T_p)\right].$$

It follows

$$\gamma_t \leq \frac{2E_b}{N_0}\sum_{l=0}^{L-1} \alpha_l^2 \mu_q^2(\epsilon_l T_p) \triangleq \sum_{l=0}^{L-1} \gamma_l^{(1)}, \quad (31)$$

Similar to the analysis by moment generating function (MGF) in [6] and using the alternative representation of the Gaussian tail function Q function in [6, p. 71], the lower bound of the average BEP is given by

$$\begin{aligned} P_e^{(1)} &= \int_0^\infty Q\left(\sqrt{\sum_{l=0}^{L-1} \gamma_l^{(1)}}\right) p\left(\gamma_l^{(1)}\right) d\gamma_l^{(1)} \\ &= \frac{1}{\pi}\int_{\theta=0}^{\pi/2} \prod_{l=0}^{L-1} \mathcal{M}_{\gamma_l^{(1)}}\left(\frac{-1}{2\sin^2\theta}\right) d\theta, \end{aligned} \quad (32)$$

with the MGF $\mathcal{M}_{\gamma_l^{(1)}}(s) \triangleq E[\exp(s\gamma_l^{(1)})]$. For the rectangular pulse and the Gaussian distributed delay error, if we define

$$a_l(\theta) \triangleq -\frac{E_b}{N_0}\frac{\alpha_l^2}{\sin^2\theta}, \quad (33)$$

$$b_l(\theta) \triangleq \frac{1}{2\sigma_{\epsilon_l}^2} + \frac{E_b}{N_0}\frac{\alpha_l^2}{\sin^2\theta}, \quad (34)$$

and

$$
\begin{aligned}
& c_l(\theta) \\
\triangleq\ & \frac{1}{\sqrt{2 b_l(\theta)}\sigma_{\epsilon_l}}\left[\Phi\left(\frac{a_l(\theta)}{\sqrt{b_l(\theta)}}\right)-\Phi\left(\frac{1}{2\sigma_{\epsilon_l}^2\sqrt{b_l(\theta)}}\right)\right] \\
& +\exp\left[-\frac{a_l(\theta)}{2\sigma_{\epsilon_l}^2 b_l(\theta)}\right]\Phi\left(\frac{1}{\sqrt{2}\sigma_{\epsilon_l}}\right), \qquad (35)
\end{aligned}
$$

and after some algebraic manipulations, we obtain

$$
\mathcal{M}_{\gamma_l^{(1)}}\left(\frac{-1}{2\sin^2\theta}\right)=c_l(\theta)\exp\left[\frac{a_l(\theta)}{2\sigma_{\epsilon_l}^2 b_l(\theta)}\right]. \qquad (36)
$$

Using the result in (32), we obtain the lower bound of the average BEP

$$
P_e^{(1)}=\frac{1}{\pi}\int_0^{\pi/2}\exp\left(\sum_{l=0}^{L-1}\frac{a_l(\theta)}{2\sigma_{\epsilon_l}^2 b_l(\theta)}\right)\prod_{l=0}^{L-1}c_l(\theta)\,d\theta. \qquad (37)
$$

2) Upper Bound: For a rectangular pulse, since $\mu_q(\epsilon_l T_p)=(1-|\epsilon_l|)$ for $|\epsilon_l|\le 1$, and

$$
\frac{\left[\sum_{l=0}^{L-1}\alpha_l^2(1-|\epsilon_l|)\right]^2}{\sum_{l=0}^{L-1}\alpha_l^2}\ge\sum_{l=0}^{L-1}\alpha_l^2(1-2|\epsilon_l|)
$$

so that

$$
\gamma_t\ge\frac{2E_b}{N_0}\sum_{l=0}^{L-1}\alpha_l^2\nu_l\triangleq\sum_{l=0}^{L-1}\gamma_l^{(2)}, \qquad (38)
$$

where

$$
\nu_l\triangleq\begin{cases}1-2|\epsilon_l|, & |\epsilon_l|\le 0.5\\ 0, & \text{else}\end{cases} \qquad (39)
$$

to ensure $\gamma_l^{(2)}=\frac{2E_b}{N_0}\alpha_l^2(1-2|\epsilon_l|)\ge 0$. Following the same derivation method as for the lower bound, we have

$$
\mathcal{M}_{\gamma_l^{(2)}}\left(\frac{-1}{2\sin^2\theta}\right)=z_l(\theta)\exp\left[\frac{x_l(\theta)}{2\sigma_{\epsilon_l}^2 y_l(\theta)}\right], \qquad (40)
$$

where

$$
x_l(\theta)\ \triangleq\ -\frac{E_b}{N_0}\frac{\alpha_l^2}{\sin^2\theta} \qquad (41)
$$

$$
y_l(\theta)\ \triangleq\ \frac{1}{2\sigma_{\epsilon_l}^2}+\frac{4E_b}{N_0}\frac{\alpha_l^2}{\sin^2\theta} \qquad (42)
$$

and

$$
\begin{aligned}
& z_l(\theta) \\
\triangleq\ & \frac{1}{\sqrt{2 y_l(\theta)}\sigma_{\epsilon_l}}\left[\Phi\left(\frac{2x_l(\theta)}{\sqrt{y_l(\theta)}}\right)-\Phi\left(\frac{1}{4\sigma_{\epsilon_l}^2\sqrt{y_l(\theta)}}\right)\right] \\
& +\exp\left[-\frac{x_l(\theta)}{2\sigma_{\epsilon_l}^2 y_l(\theta)}\right]\Phi\left(\frac{1}{2\sqrt{2}\sigma_{\epsilon_l}}\right). \qquad (43)
\end{aligned}
$$

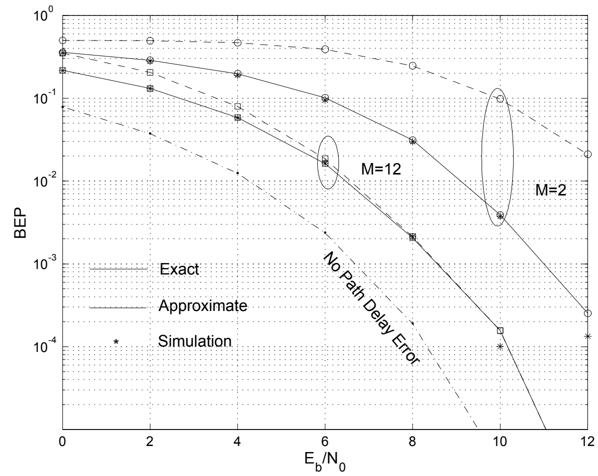

Fig. 3. Comparison of BEP for Rake receivers in the presence of delay errors using exact and approximate expressions with simulation. M is the number of pilot symbols.

Finally, we obtain the upper bound of the BEP expressed as an integral with finite limits

$$
P_e^{(2)}=\frac{1}{\pi}\int_{\theta=0}^{\pi/2}\exp\left(\sum_{l=0}^{L-1}\frac{x_l(\theta)}{2\sigma_{\epsilon_l}^2 y_l(\theta)}\right)\prod_{l=0}^{L-1}z_l(\theta)\,d\theta. \qquad (44)
$$

IV. Numerical Evaluation

In this section, we evaluate the BEP of Rake receivers in the presence of channel estimation errors, and compare the analytical results with the Monte Carlo numerical simulation. The path delays are assumed $\tau_l = 4lT_p$, $1\le l\le L=8$. The power delay profile is given by $\Omega_l=\Omega_0\exp(-l\delta)$, where Ω_0 normalizes the total power to unity, and the decay factor δ is assumed of 0.02 [6, p. 27],[16]. The path gain is $\alpha_l=\sqrt{\Omega_l}$.

Fig. 3 demonstrates that the BEP obtained by the exact expression matches well with the Monte Carlo simulation. By observing the E_b/N_0 difference with that without errors, we conclude that the channel path delay error has diminished the capability of the Rake receiver to capture the multipath diversity. We also compare the exact and the approximate BEP expressions as a function of the number of pilot symbols. The approximate BEP converges to the true BEP for high SNR.

The upper and lower bounds are compared with simulations in Fig. 4. The lower bound is tighter than the upper bound, in particular for a larger number of pilot symbols ($M = 12$). With a small number of pilot symbol, both bounds become loose.

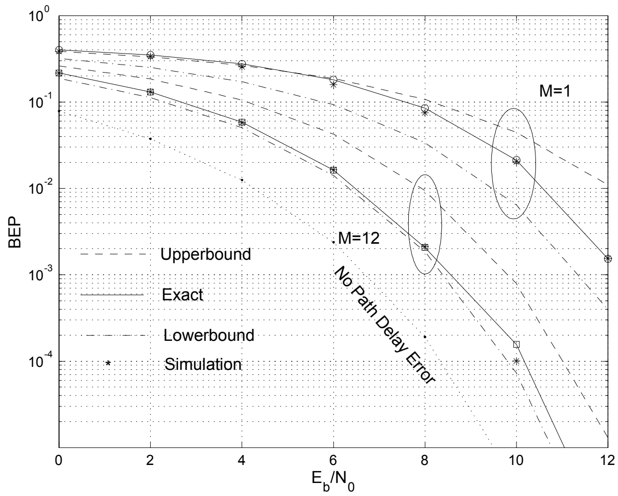

Fig. 4. The upper and lower bounds of BEP are compared with that using the exact expression for an MRC Rake in the presence of channel delay estimation errors. M is the number of pilot symbols.

V. Conclusion

The effect of the channel path delay estimate error has been investigated for an impulse radio UWB Rake receiver using MRC. Both misalignment and missing-path errors are accounted for. An exact expression of the BEP is obtained. An approximate and upper/lower bounds are also obtained. Simulation results are in close match with the analytical results. The channel path delay error is shown to diminish the capability of the Rake receiver to capture the multipath diversity.

References

[1] M. Z. Win and R. A. Scholtz, "On the energy capture of ultra-wide bandwidth signals in dense multipath environments," *IEEE Commun. Lett.*, vol. 2, no. 9, pp. 245–247, Sept. 1998.

[2] J. Ianniello, "Time delay estimation via cross-correlation in the presence of large estimation errors," *IEEE Trans. Acous., Speech, and Signal Processing*, vol. ASSP-30, no. 6, pp. 998–1003, Dec. 1982.

[3] W. Lovelace and J. K. Townsend, "The effects of timing jitter and tracking on the performance of impulse radio," *IEEE J. Select. Areas Commun.*, vol. 20, no. 9, pp. 1646–1651, Dec. 2002.

[4] I. Guvenc and H. Arslan, "Performance evaluation of UWB systems in the presence of timing jitter," in *Proc. IEEE Conference on Ultra Wideband Systems and Technologies (UWBST'03)*, Reston, Virginia, Nov. 2003.

[5] A. H. Quazi, "An overview on the time delay estimate in active and passive systems for target localization," *IEEE Trans. Acous., Speech, and Signal Processing*, vol. ASSP-29, no. 3, pp. 527–533, June 1981.

[6] M. K. Simon and M.-S. Alouini, *Digital Communication over Fading Channels: a Unified Approach to Performance Analysis*. John Wiley & Sons, Inc., 2000.

[7] V. Lottici, A. D'Andrea, and U. Mengali, "Channel estimation for ultra-wideband communications," *IEEE J. Select. Areas Commun.*, vol. 20, no. 9, pp. 1638–1645, Dec. 2002.

[8] J. Panicker and S. Kumar, "Effect of system imperfections on BER performance of a CDMA receiver with multipath diversity combining," *IEEE Trans. Veh. Technol.*, vol. 45, no. 4, pp. 622–630, Nov. 1996.

[9] S. M. Kay, *Fundamentals of Statistical Signal Processing: Estimation Theory*. Upper Saddle River, New Jersey: Prentice-Hall, 1993.

[10] Q. T. Zhang, "Probability of error for equal-gain combiners over Rayleigh channels: some closed-form solutions," *IEEE Trans. Commun.*, vol. 45, no. 3, pp. 270–273, Mar. 1997.

[11] N. N. Lebedev, *Special Functions and Their Applications*. New York: Dover Publications, Inc., 1972.

[12] I. S. Gradshteyn and I. M. Ryzhik, *Table of Integrals, Series, and Products*, 5th ed. New York: Academic, 1980.

[13] P. J. Davis and P. Rabinowitz, *Methods of Numerical Integration*, 2nd ed. London: Academic Press, Inc., 1984.

[14] M. Abramowitz and I. A. Stegun, Eds., *Handbook of Mathematical Functions with Formulas, Graphs, and Mathematical Tables*, 10th ed. Government Printing Office, 1972.

[15] Y. Yin, J. P. Fonseka, and I. Korn, "Sensitivity to timing errors in EGC and MRC techniques," *IEEE Trans. Commun.*, vol. 51, no. 4, pp. 530–534, Apr. 2003.

[16] J. R. Foerster, "The effects of multipath interference on the performance of UWB systems in an indoor wireless channel," in *Proc. IEEE VTS 53rd Vehicular Technology Conf. (VTC Spring'01)*, vol. 2, May 2001, pp. 1176–1180.